ASTRONOMY & ASTROPHYSICS
SUPPLEMENT SERIES

JUNE II **1998**, PAGE 449

Astron. Astrophys. Suppl. Ser. **130**, 449–454 (1998)

The thicknesses and inclinations of 71 northern spiral galaxies

Jun Ma[1,2,3], Qiu-He Peng[1], and Qiu-Sheng Gu[1,2]

[1] Department of Astronomy, Nanjing University, Nanjing, 210093, China
[2] United Lab. for Optical Astronomy, The Chinese Academy of Sciences, China
[3] Shanghai Astronomical Observatory, the Chinese Academy of Sciences, Shanghai 200030, China

Received September 23, 1997; accepted January 5, 1998

Abstract. This paper presents the thicknesses and inclinations (i.e., the angle between the galactic plane and the tangent plane) of 71 northern spiral galaxies. The method for measuring the thickness has been proposed by Peng. It is based on the solution of Poisson's equation for a logarithmic disturbance of density. The inclination is determined by assuming that the pattern of spiral structure is a logarithmic spiral. We find that the thickness is correlated with color and with the H_α + [NII] equivalent width.

Key words: galaxies: spiral; structure; kinematics and dynamics; fundamental parameters

1. Introduction

There are two approaches to estimate the thickness of a galactic disc. One, for edge-on spirals, has been suggested by van der Kruit & Searle (1981a,b, 1982a,b), and is based on surface photometry. The other one, for non-edge-on galaxies, has been proposed by Peng (1988). It is based on the solution of Poisson's equation for a logarithmic disturbance of density. The latter is effective and simple as long as spiral arms are distinguishable on the images.

The inclination of a galaxy (i.e., the angle between the galactic plane and the tangent plane) is difficult to determine. It has been shown by Danver (1942) and Kennicutt & Hodge (1982) that the spiral arm can be represented by a logarithmic spiral form with constant pitch angle μ. The inclination can be determined by comparing the fitted spiral curve with the image.

In this paper, we present the thicknesses and inclinations for 71 northern spiral galaxies which are selected from more than 600 ones whose images are taken from the Digitized Sky Survey[1]. Most galaxies in this paper are grand design spiral ones with Arm Classification ≥ 5 (Elmegreen & Elmegreen 1987) except for six spirals. Usually there are two arms for most galaxies, the arm closest to the center is used for measurement.

The structure of this paper is as following: In Sect. 2, we outline the steps how to measure the thickness, determine the inclination, and select the samples. In Sect. 3, we present the results and discuss errors. We discuss statistical properties in Sect. 4.

2. Main steps of the method, and choice of the sample

The main steps are:

(1). Find the position of the innermost point of a spiral arm and measuring its coordinate (ρ_0, θ_0) relative to the image center and to the major axis.

(2). Vary the value of the inclination γ around $\arccos(d_{25}/D_{25})$ and fit the spiral arm starting from that innermost point with a logarithmic spiral curve to get its winding parameter Λ such that $\mu = \arctan(m/\Lambda)$, where m is the number of arms, with a least square method. D_{25} and d_{25} are taken from the Third Catalog of Bright Galaxies by de Vaucouleurs et al. (1991, RC3). They are the apparent major and minor isophotal diameters measured at or reduced to the surface brightness level $\mu_B = 25.0$ blue mag per square arc second.

(3). Determine the inclination and the corresponding winding parameter by comparing the fitted spiral curve with the image.

(4). Calculate the thickness of the galactic disk h, by

$$h = \frac{2r_0}{\sqrt{m^2 + \Lambda^2}}, \quad (1)$$

Send offprint requests to: Jun Ma, e-mail: qhpeng@nju.edu.cn

[1] Based on photographic data of the National Geographic Society – Palomar Observatory Sky Survey (NGS-POSS) obtained using the Oschin Telescope Palomar Mountain. The NGS-POSS was funded by a grant from the National Geographic Society to the California Institute of Technology. The plates were processed into the present compressed digital form with their permission. The Digitized Sky Survey was produced at the Space Telescope Science Institute under US Government grant NAG W-2166.

$$r_0 = \frac{\rho_0 \sqrt{\sin^2 \theta_0 + \cos^2 \theta_0 \cos^2 \gamma}}{\cos \gamma}, \quad (2)$$

where m is the number of the arms (see Peng 1988).

(5). The thickness of the galactic disk, H in kpc, is

$$H = hd, \quad (3)$$

where d is the distance of the galaxy

$$d = \frac{v_{\rm opt}}{H_0}, \quad (4)$$

where H_0 is the Hubble constant taken as 75 km/s/Mpc, and $v_{\rm opt}$, the mean heliocentric radial velocity in km/s derived from optical observations, is taken from the RC3.

Our statistical sample contains 71 galaxies, selected from more than 600 northern spirals having a determined $(B-V)^0_{\rm T}$ (i.e., the total color index corrected for galactic and internal extinction and redshift) in RC3 according to one single criterion: their images have distinguishable spiral arms. The mean Hubble type indexes (T) of these galaxies are from 2 to 6, and they have $\log(D_{25}/d_{25})$ less than 0.76.

Our data reduction and analyses were done with IRAF[2] installed in the Sun Workstation at the Laboratory of Astronomical Data Analysis of Nanjing University.

3. Results and errors

The thicknesses (H), inclinations (γ) and winding parameters (Λ) of 71 northern spiral galaxies are listed in Tables 1 and 2. Some other parameters are also listed: m is the number of arms, T the mean numerical Hubble stage index, μ ($= \arctan(m/\Lambda)$) the pitch angle of a spiral arm, h the apparent thickness, d the distance, H/D_0 the flatness, D_0 is the isophotal major diameter corrected to the "face-on" ($\gamma = 0°$), and for Galactic extinction, but not for redshift.

The errors arise mainly from: a) the position of the innermost point for the arm; b) the inclination of the galaxy; c) the position of the galactic center. The errors from b) and c), however, can be reduced if we properly modify the grey-scale of the image by using IRAF to obtain the fine structure of the galaxy as deeply as possible. The estimations of error are derived from the formulae given by Peng (1988).

4. Statistical property

4.1. Dependence on color

Figures 1 and 2 present the correlations between the flatness (H/D_0) and thickness (H) and galaxy color ($(B-V)^0_{\rm T}$). The integrated colors of disk galaxies are predominantly influenced by their star formation history (Searle et al. 1973), and the strong correlations observed between color and flatness or thickness point to a coupling between the flatness or thickness and the integrated star formation history of galaxies.

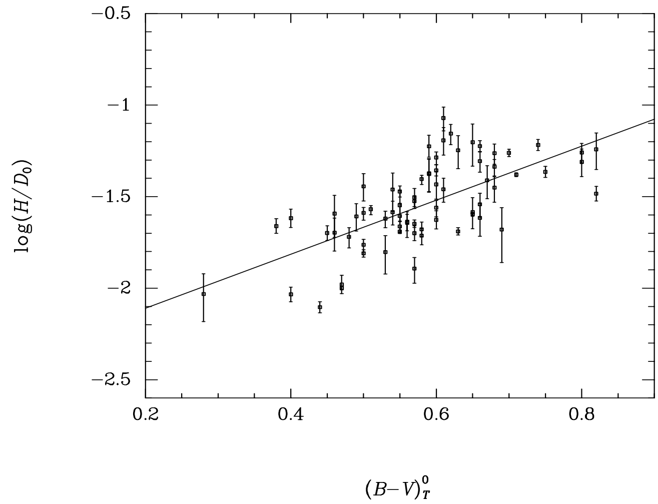

Fig. 1. Flatness of spiral galaxy plotted versus the corrected $B-V$ color

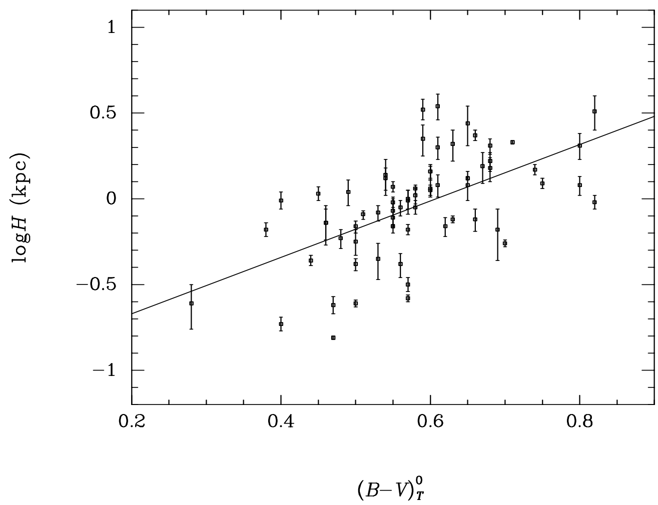

Fig. 2. Thickness of spiral galaxy plotted versus the corrected $B-V$ color

Figure 3 plots flatness as a function of the corrected $U-B$ color ($(U-B)^0_{\rm T}$), which are taken from RC3, the total $U-B$ color index corrected for differential galactic and internal extinction (to "face-on") and for redshift. The dependence of thickness on $(U-B)^0_{\rm T}$ is illustrated in Fig. 4.

[2] IRAF is distributed by the National Optical Astronomy Observatories, which is operated by the Association of Universities for Research in Astronomy, Inc., under cooperative agreement with the National Science Foundation.

Table 1. Thicknesses and inclinations of 71 northern spiral galaxies

PGC	Names	m	T	γ (°)	$\Lambda \pm d\Lambda/\Lambda$	μ (°)	$h \pm dh/h$ (′)	d (Mpc)	$H \pm dH/H$ (kpc)	H/D_0
PGC 1405	NGC 91	2	5.0	45.5	4.70±18.1%	23.1	0.077±20.1%	68.97	1.54±20.1%	0.039
PGC 2901	NGC 266	2	2.0	12.2	8.91±23.0%	12.7	0.177±22.6%	62.43	3.21±22.6%	0.057
PGC 5139	NGC 514	2	5.0	37.4	4.17±7.7%	25.6	0.085±10.0%	33.69	0.83±10.0%	0.024
PGC 5818	NGC 598	2	6.0	48.9	4.26±4.3%	25.2	0.743±2.8%	0.72*	0.16±2.8%	0.010
PGC 6624	NGC 673	2	5.0	47.1	6.47±13.1%	17.2	0.054±16.8%	69.88	1.10±16.8%	0.025
PGC 6799	NGC 688	2	3.2	57.9	15.06±25.7%	7.6	0.087±23.8%	54.81	1.39±23.8%	0.035
PGC 7282	NGC 735	2	3.0	67.1	7.33±18.8%	15.3	0.066±15.7%	63.19	1.21±15.7%	0.035
PGC 10329	NGC 1073	2	5.0	24.2	32.05±12.6%	3.6	0.051±11.3%	16.12	0.24±11.3%	0.010
PGC 10932	IC 267	2	3.0	34.1	14.39±13.3%	7.9	0.119±13.4%	47.69	1.65±13.4%	0.055
PGC 13826	IC 342	2	6.0	12.2	9.37±1.2%	12.0	0.220±1.7%	3.30**	0.21±1.7%	0.005
PGC 15212	A0423+70	2	4.0	64.2	4.54±16.3%	23.8	0.063±25.4%	39.29	0.72±25.4%	0.026
PGC 15867	NGC 1642	2	5.0	0.0	6.45±16.6%	17.2	0.072±16.4%			0.037
PGC 17625	NGC 1961	2	5.0	54.2	19.86±17.3%	5.7	0.064±16.0%	53.11	0.99±16.0%	0.013
PGC 20222	NGC 2339	2	4.0	37.7	18.47±23.4%	6.2	0.049±23.3%	31.48	0.45±23.3%	0.016
PGC 21832	A0743+59	2	3.0	65.7	7.46±20.9%	15.0	0.089±20.6%	86.77	2.25±20.6%	0.042
PGC 22031	NGC 2441	2	3.0	33.1	10.94±7.2%	10.4	0.088±6.5%	47.87	1.22±6.5%	0.043
PGC 22957	NGC 2535	2	5.0	30.7	4.92±9.7%	22.1	0.062±11.2%	54.39	0.98±11.2%	0.024
PGC 23630	NGC 2582	2	2.0	27.0	5.86±14.3%	18.8	0.069±13.5%	59.48	1.19±13.5%	0.055
PGC 24996	IC 2421	2	5.0	21.1	7.39±8.7%	15.2	0.052±10.1%	58.52	0.88±10.1%	0.023
PGC 25946	NGC 2776	2	5.0	32.0	8.04±9.3%	14.0	0.058±12.1%	34.91	0.59±12.1%	0.019
PGC 26666	NGC 2857	2	5.0	17.0	8.42±6.9%	13.4	0.047±8.7%	64.85	0.89±8.7%	0.021
PGC 27077	NGC 2903	2	4.0	53.4	9.05±19.6%	12.5	0.357±19.1%	7.53	0.78±19.1%	0.028
PGC 28196	NGC 2998	2	5.0	62.4	9.93±10.7%	11.4	0.058±9.3%	63.56	1.07±9.3%	0.020
PGC 28617	NGC 3055	2	5.0	46.9	11.71±16.9%	9.7	0.077±17.2%	25.07	0.56±17.2%	0.036
PGC 28630	NGC 3031	2	2.0	57.3	8.27±7.9%	13.6	0.904±8.5%	3.60*	0.95±8.5%	0.033
PGC 30087	NGC 3184	2	6.0	21.1	5.54±3.8%	19.8	0.167±5.3%	5.39	0.26±5.3%	0.022
PGC 31883	NGC 3338	2	5.0	54.9	7.93±6.1%	14.2	0.163±5.7%	17.29	0.82±5.7%	0.027
PGC 31968	NGC 3344	2	4.0	0.0	9.06±9.2%	12.4	0.141±9.1%	7.67	0.31±9.1%	0.020
PGC 34695	NGC 3627	2	3.0	62.8	5.82±7.3%	19.0	0.410±7.3%	9.37	1.12±7.3%	0.044
PGC 34767	NGC 3631	2	5.0	22.3	6.50±5.0%	17.1	0.150±6.4%	15.24	0.66±6.4%	0.030
PGC 35105	A1122+64	2	5.0	10.0	6.41±8.0%	17.3	0.046±8.8%	49.65	0.66±8.8%	0.022
PGC 36243	NGC 3810	2	5.0	49.9	10.84±9.6%	10.5	0.113±7.8%	12.77	0.42±7.8%	0.026
PGC 36446	NGC 3832	2	4.0	30.7	6.88±13.4%	16.2	0.070±14.4%	92.08	1.87±14.4%	0.036
PGC 36604	NGC 3861	2	3.0	56.7	11.03±12.6%	10.3	0.105±10.8%	67.57	2.06±10.8%	0.046
PGC 36902	NGC 3897	2	4.0	27.0	6.91±7.8%	16.1	0.046±11.1%	85.79	1.15±11.1%	0.024
PGC 37229	NGC 3938	2	5.0	0.0	8.36±4.1%	13.4	0.083±4.0%	10.28	0.25±4.0%	0.015
PGC 37306	NGC 3953	2	4.0	59.9	7.74±14.2%	14.5	0.198±14.7%	13.16	0.76±14.7%	0.029
PGC 37386	NGC 3963	2	4.0	24.2	7.75±16.6%	14.5	0.068±18.7%	42.72	0.84±18.7%	0.025
PGC 37617	NGC 3992	2	4.0	58.5	15.69±36.3%	7.3	0.162±33.3%	14.12	0.67±33.3%	0.021
PGC 38024	A1200+41	2	4.0	54.4	6.26±9.2%	17.7	0.056±14.9%	81.83	1.33±14.9%	0.026
PGC 39028	NGC 4192	2	2.0	73.6	14.35±24.5%	7.9	0.421±20.4%			0.042
PGC 39483	IC 3115	2	6.0	35.6	5.86±13.8%	18.8	0.086±13.3%			0.049
PGC 39600	NGC 4258	2	4.0	70.6	5.91±9.2%	18.7	0.627±7.5%	6.40	1.17±7.5%	0.034
PGC 39964	A1219+41	2	3.0	31.7	12.33±17.2%	9.2	0.076±16.5%	92.36	2.04±16.5%	0.049
PGC 40001	NGC 4303	2	4.0	22.0	8.35±8.2%	13.5	0.111±8.3%	21.43	0.69±8.3%	0.017
PGC 40153	NGC 4321	2	4.0	30.4	7.90±20.1%	14.2	0.197±19.0%	21.05	1.21±19.0%	0.026

4.2. Dependence on Hubble type

The tightness of the spiral pattern, in addition to the disk resolution and bulge-to-disk ratio, are the fundamental criteria in Hubble's (1926) classification of spirals. It is interesting to see the dependence of flatness on the Hubble type, which is shown in Fig. 5. The flatness of a spiral galaxy decreases smoothly an average along the Hubble sequence, but the dispersion in flatness among galaxies of the same Hubble type is very large. Figure 6 shows the correlation between thickness and the Hubble sequence.

Table 2. Thicknesses and inclinations of 71 northern spiral galaxies

PGC	Names	m	T	γ (°)	$\Lambda \pm \mathrm{d}\Lambda/\Lambda$	μ (°)	$h \pm \mathrm{d}h/h$ (′)	d (Mpc)	$H \pm \mathrm{d}H/H$ (kpc)	H/D_0
PGC 40695	NGC 4411A	2	5.0	29.3	9.57±4.3%	11.8	0.112±4.1%	16.96	0.55±4.1%	0.055
PGC 41812	NGC 4535	2	5.0	25.9	10.60±9.6%	10.7	0.137±10.0%	26.31	1.05±10.0%	0.019
PGC 42741	NGC 4639	2	4.0	52.5	8.53±14.2%	13.2	0.197±13.0%	11.97	0.69±13.0%	0.070
PGC 45658	NGC 5000	2	4.0	31.7	8.95±22.2%	12.6	0.096±21.4%	75.61	2.11±21.4%	0.057
PGC 45948	NGC 5033	2	5.0	70.1	18.32±24.2%	6.2	0.215±21.4%	11.48	0.72±21.4%	0.020
PGC 47067	A1324+20	2	4.0	37.4	9.99±9.4%	11.3	0.036±12.4%	95.25	1.00±12.4%	0.031
PGC 49514	NGC 5371	2	4.0	57.4	9.48±27.7%	11.9	0.274±26.4%	34.33	2.74±26.4%	0.063
PGC 49555	NGC 5364	2	4.0	49.8	13.48±2.6%	8.4	0.141±2.3%	16.89	0.69±2.3%	0.020
PGC 49952	NGC 5409	2	3.0	41.9	23.41±21.1%	4.9	0.042±20.1%			0.024
PGC 50063	NGC 5457	2	6.0	41.1	8.24±4.7%	13.6	0.227±7.0%	6.90***	0.44±7.0%	0.008
PGC 52641	NGC 5740	2	3.0	59.1	11.61±17.9%	9.8	0.069±15.9%	20.89	0.42±15.9%	0.023
PGC 54001	NGC 5859	2	4.0	71.6	6.75±16.0%	16.5	0.189±17.4%	62.49	3.43±17.4%	0.064
PGC 54849	NGC 5921	2	4.0	45.6	6.05±8.3%	18.3	0.253±7.9%	19.43	1.43±7.9%	0.052
PGC 55725	NGC 5985	2	3.0	62.4	11.37±2.7%	10.0	0.139±3.2%	32.89	1.33±3.2%	0.025
PGC 60459	NGC 6384	2	4.0	53.6	9.23±6.5%	12.2	0.147±6.5%	22.53	0.96±6.5%	0.022
PGC 60635	IC 1267	2	3.0	57.5	6.64±13.3%	16.8	0.092±13.9%	124.15	3.32±13.9%	0.060
PGC 65001	NGC 6946	2	6.0	46.7	5.54±6.2%	19.8	0.154±8.8%	4.20**	0.19±8.8%	0.009
PGC 65086	NGC 6951	2	4.0	46.7	4.20±7.9%	25.4	0.289±6.0%	17.75	1.49±6.0%	0.060
PGC 65375	NGC 6962	2	2.0	55.4	11.40±2.9%	10.0	0.129±2.9%	56.72	2.13±2.9%	0.042
PGC 68110	A2206+40	2	4.0	36.8	2.94±11.9%	34.2	0.074±16.1%	70.84	1.52±16.1%	0.035
PGC 69327	NGC 7331	2	3.0	72.6	9.60±6.3%	11.8	0.234±4.2%	11.13	0.76±4.2%	0.020
PGC 70144	A2255+02	2	5.0	24.2	5.39±5.4%	20.3	0.060±5.9%	65.23	1.14±5.9%	0.039
PGC 70291	NGC 7463	2	3.0	76.4	30.24±32.3%	3.8	0.027±30.0%	30.96	0.24±30.0%	0.009
PGC 70419	NGC 7479	2	5.0	54.7	10.60±7.8%	10.7	0.255±7.3%	31.92	2.37±7.3%	0.060
PGC 71517	NGC 7677	2	3.5	61.9	5.74±18.2%	19.2	0.141±15.5%	48.15	1.97±15.5%	0.085

* The distance is taken from Faber & Gallagher (1979).
** The distance is taken from Lang (1983).
*** The distance is taken from Roberts et al. (1975).

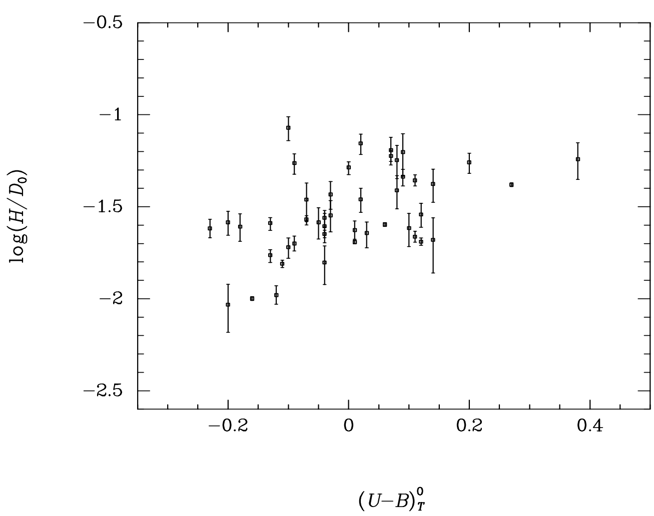

Fig. 3. Flatness of spiral galaxy plotted versus the corrected $U-B$ color

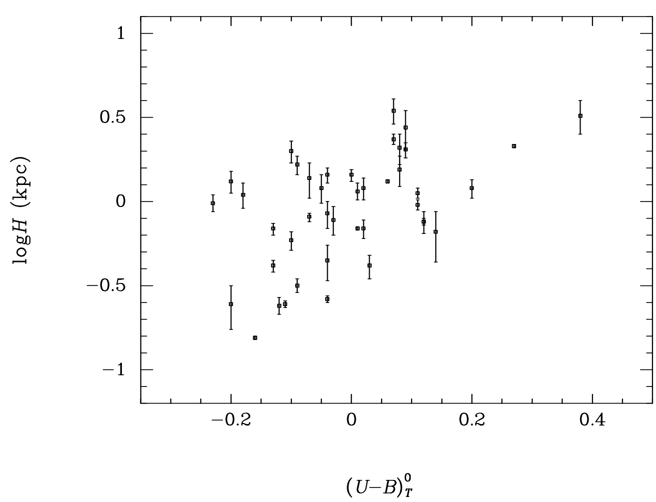

Fig. 4. Thickness of spiral galaxy plotted versus the corrected $U-B$ color

4.3. Correlation between H_α + [NII] *equivalent width and thickness*

Kennicutt & Kent (1983) presented the combined results of photometric and spectrophotometric surveys of H_α emission for 200 field and Virgo cluster galaxies. Romanishin (1990) published large aperture photometric measurement of H_α + [NII] emission line strengths of 110 spiral galaxies. We have measured the thicknesses of some

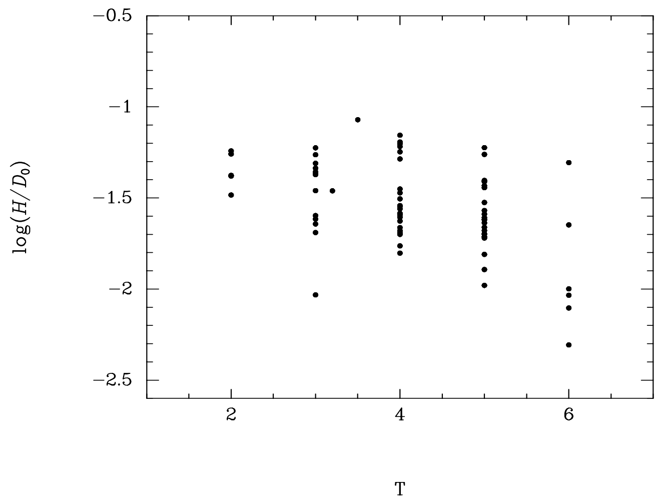

Fig. 5. Flatness of spiral galaxy plotted versus the Hubble sequence

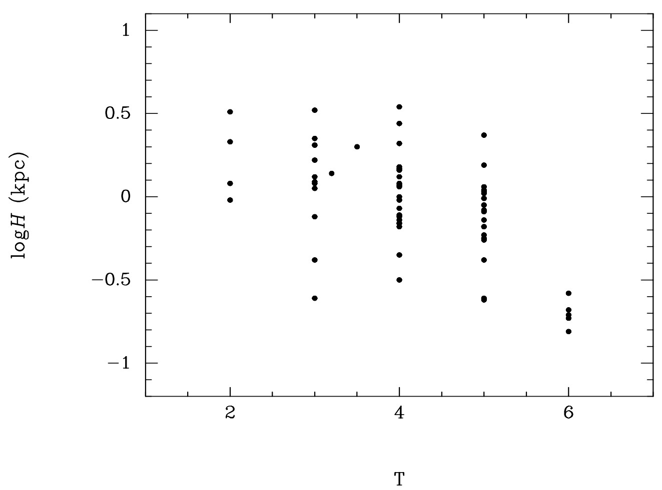

Fig. 6. Thickness of spiral galaxy plotted versus the the Hubble sequence

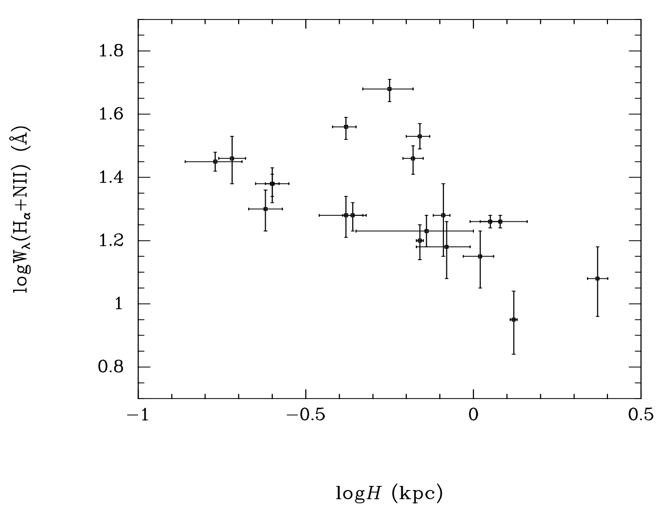

Fig. 7. H_α + [NII] emission line plotted versus the thickness

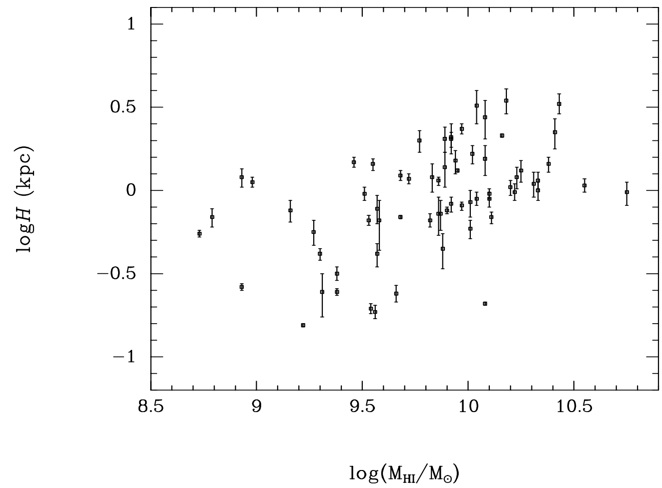

Fig. 8. Thickness of spiral galaxy plotted versus the Neutral hydrogen masses

Table 3. H_α + [NII] equivalent width and thickness

PGC	Names	T	$H \pm \mathrm{d}H/H$ (kpc)	EW (Å)
PGC 5974	NGC 628	5.0	0.25±27%	24±2
PGC 10329	NGC 1073	5.0	0.24±11.3%	20±3
PGC 28617	NGC 3055	5.0	0.56±17.2%	48±4
PGC 31883	NGC 3338	5.0	0.82±5.7%	19±5
PGC 34695	NGC 3627	3.0	1.12±7.3%	18±1
PGC 34767	NGC 3631	5.0	0.66±6.4%	29±3
PGC 36243	NGC 3810	5.0	0.42±7.8%	36±3
PGC 37229	NGC 3938	5.0	0.25±4.0%	24±3
PGC 37386	NGC 3963	4.0	0.84±18.7%	15±3
PGC 40001	NGC 4303	4.0	0.69±8.3%	34±3
PGC 40153	NGC 4321	4.0	1.21±19.0%	18±1
PGC 41812	NGC 4535	5.0	1.05±10.0%	14±3
PGC 45948	NGC 5033	5.0	0.72±21.4%	17±2
PGC 47404	NGC 5194	4.0	0.17±16%	28±2
PGC 49555	NGC 5364	4.0	0.69±2.3%	16±2
PGC 50063	NGC 5457	6.0	0.44±7.0%	19±2
PGC 52641	NGC 5740	3.0	0.42±15.9%	19±3
PGC 55725	NGC 5985	3.0	1.33±3.2%	8.9±2
PGC 65001	NGC 6946	6.0	0.19±7.0%	29±5
PGC 70419	NGC 7479	5.0	2.37±7.3%	12±3

spirals observed by them. The results are listed in Table 3. We use the formula (Romanishin 1990):

EW (Romanishin's) = 1.22 × EW(KK's)

Figure 7 shows the correlation of H_α + [NII] equivalent width with the thickness. There might be a negative correlation between star formation activity and thickness of a galaxy, but the scatter is large and there are only 20 samples. The thicknesses of NGC 628 and NGC 5194 are from Peng's paper (Peng 1988).

Figure 8 plots the relation between thickness and neutral hydrogen masses. The neutral hydrogen mass is derived by de Vaucouleurs et al. (1991, RC3),

$$\log(M_{\mathrm{HI}}/M_\odot) = 5.696 + (16.6 - m^\circ_{21})/2.5 + 2.0 \times \log d \quad (5)$$

where m°_{21}, from RC3, is the 21-cm emission line magnitude and corrected for self-absorption and d, in Mpc, is the distance of a galaxy.

Figure 8 suggests that a thicker galaxy contains more neutral hydrogen, although the dispersion is large.

Acknowledgements. We would like to thank Prof. Jiehao Huang for his help in finishing this paper. We also thank Prof. Jingyao Hu for his hospitality and discussion at the Xinglong Observational Station of Beijing Observatory, and are grateful to Rui Chen, Zhaohui Ji and Zhaohui Shang for their help. We wish to thank Prof. Zongyun Li for a valuable discussion. This work is supported by the National Nature Science Foundation, the National Grand Project "Climbing Up" of China and the Doctoral Program Foundation of State Education Commission of China.

References

Danver C.C., 1942, Ann. Obs. Lund. No. 10
de Vaucouleurs G., de Vaucouleurs A., Corwin H.G., Buta B.J., Fouque P., 1991, the Third Reference Catalog of Bright Galaxies. New York: Springer-Verlag
Elmegreen D.M., Elmegreen B.G., 1987, ApJ 314, 3
Faber S.M., Gallagher J.S., 1979, ARA&A 17, 135
Hubble E.P., 1926, ApJ 64, 321
Kennicutt R.C., Hodge P., 1982, ApJ 253, 101
Kennicutt R.C., Kent S.M., 1983, AJ 88, 1094
Lang K.R., 1980, Astrophysical Formulae. Springer-Verlag
Peng Qiu-he, 1988, A&A 206, 18
Roberts W.W., Roberts M.S., Shu F.H., 1975, ApJ 196, 381
Romanishin W., 1990, AJ 100, 373
Searle L., Sargent W.L.W., Bagnuolo W.G., 1973, ApJ 179, 427
van der Kruit P.C., Searle L., 1981a, A&A 95, 105
van der Kruit P.C., Searle L., 1981b, A&A 95, 116
van der Kruit P.C., Searle L., 1982a, A&A 110, 61
van der Kruit P.C., Searle L., 1982b, A&A 110, 79